

# Supporting Information: Tip-Enhanced Raman Detection of Antibody Conjugated Nanoparticles on Cellular Membranes.

Kristen D. Alexander and Zachary D. Schultz\*

University of Notre Dame, Department of Chemistry and Biochemistry, Notre Dame, IN, 46556

\*Corresponding author: Schultz.41@nd.edu

## **Abstract:**

This supplement contains extensive descriptions of the experimental techniques, instrumentation, and procedures in the section entitled Materials and Methods (pp S-2 – S-4). We have included hyperspectral characterization of conjugated nanoparticles and Raman spectra obtained in the absence of cellular membranes, including Figure S1 (pp S-7) and Figure S2 (pp S-8). We have further included the computational results of the expected enhancement associated with scanning the nanoparticle tip 20 nm above and below the nanoparticle on the sample (pp S-10). These materials are intended to provide a more complete understanding of the work reported in our manuscript.

## **Materials and Methods:**

### Preparation of conjugated Nanoparticles

50 nm Au nanoparticles were conjugated with an antibody for human IgG via EDC coupling chemistry using the nanoparticle conjugation kit available from Nanopartz (21-PC-Kit1). 5  $\mu$ L anti-IgG was added to a 1 mL volume of carboxylated Au nanoparticle colloid and vortexed for 1 minute. Next, 5  $\mu$ L of 3.2 mM aqueous EDC solution was added and the solution was vortexed for 1 hour. After vortexing, the resulting mixture was centrifuged at 4000 rpm for 30 minutes, causing the nanoparticles to form a compact pellet at the bottom of the microcentrifuge tube. The supernatant was removed and the nanoparticles were resuspended in 1.5 mL PBS. The latter two steps were repeated two more times to ensure that all of the free EDC and anti-IgG molecules were removed from the solution.

Cells were labeled with the conjugated nanoparticles by adding a 100  $\mu$ L aliquot of conjugated nanoparticle solution drop-wise onto a glass slide plated with SW480 colon cancer cells and allowed to sit. Colon cancer cells were used for convenience and the specific cell line is not a factor in these experiments. The glass slide was then gently rinsed with deionized water and the cells were fixed in -20 °C methanol overnight. The fixed cells were dried prior to further experiments.

### TERS Microscopy

TERS microscopy was performed on cells with anti-IgG Au nanoparticles affixed as described above. The TERS microscope has been described previously.<sup>1</sup> Briefly, the instrument utilizes an upright microscope with a phase-feedback AFM (Nanonics MV4000) situated to place the AFM tip at the focus of an upright microscope. Raman excitation consisted of a 35 mW continuous wave HeNe laser. The TERS tip was comprised of a cantilevered glass filament with a 100- 150 nm Au nanoparticle at the apex (Nanonics Supertips, LTD). The tip size was specified by the manufacturer and used as received. The nanoparticle tip was irradiated with 0.5 -1.5 mW of laser power, and we simultaneously recorded both topographical and tip enhanced Raman maps of our sample. As a means of avoiding polarization artifacts associated with linearly polarized light in the backscattering geometry,<sup>2</sup> radial polarization was employed using a liquid crystalline mode converter (ArcOptix). The backscattered Raman signal was then episcattered through the 100×, 0.7 NA, objective and sent to a spectrometer (Jobin Yvon, iHR320), equipped with a 600 grooves mm<sup>-1</sup> grating to disperse the signal onto a CCD camera (Jobin Yvon, Synapse). Raman spectra were obtained using a 1 s acquisition period and with a spatial interval as small as 20 nm.

### Dark Field Microscopy

Dark Field microscopy was obtained with two different microscopes. The TERS microscope is equipped with reflective dark-field illumination using an Olympus LMPlan FLN 50x 0.5 BD objective and a 150W tungsten halogen lamp, which enables identification of plasmonic particles on the cells.

Hyperspectral dark field microscopy was performed using a CytoViva microscope. This microscope consists of a 150W aluminum halogen lamp coupled into the CytoViva darkfield illumination system. Scattered light was collected by a 40x, 0.6 NA fluorite objective on a standard Olympus BX series microscope. Spectra were collected from 400-1000 nm using a spectrograph and integrated Cooke pixelfly CCD. The stage was stepped in 10 nm increments. The stage, CCD and imaging setup are controlled via middleware integrated into ENVI (ITT Visual Information Solutions). Data analysis was also performed using ENVI.

### FEM Calculations

Finite element method (FEM) calculations were performed using COMSOL version 3.5a. The initial study consisted of a single 50 nm Au nanoparticle dimer embedded in a medium with a dielectric constant  $n=1$ . The dielectric properties for Au at 632.8 nm were obtained from Johnson and Christy.<sup>3</sup> The electric field was modeled to propagate along the  $z$ -axis at a wavelength 632.8 nm. Here, it is important to note that, the expression describing radial polarization includes an integral that has no closed form solution and, therefore, cannot easily be modeled by COMSOL. Because we are only interested in the scattered electric field in the immediate vicinity of the nanoparticle, we approximate the electric field at the focus by modeling polarization components of equal magnitude along the  $x$ ,  $y$  and  $z$ -axes. This approximation is consistent with previous reports of the relative polarization contributions for a radial polarized beam focused at an intermediate NA.<sup>4</sup> Tip scanning models were generated from calculations of the scattered electric field including a second nanoparticle positioned at distances representative of the TERS measurements.

## **Supporting Results:**

### Nanoparticle Characterization:

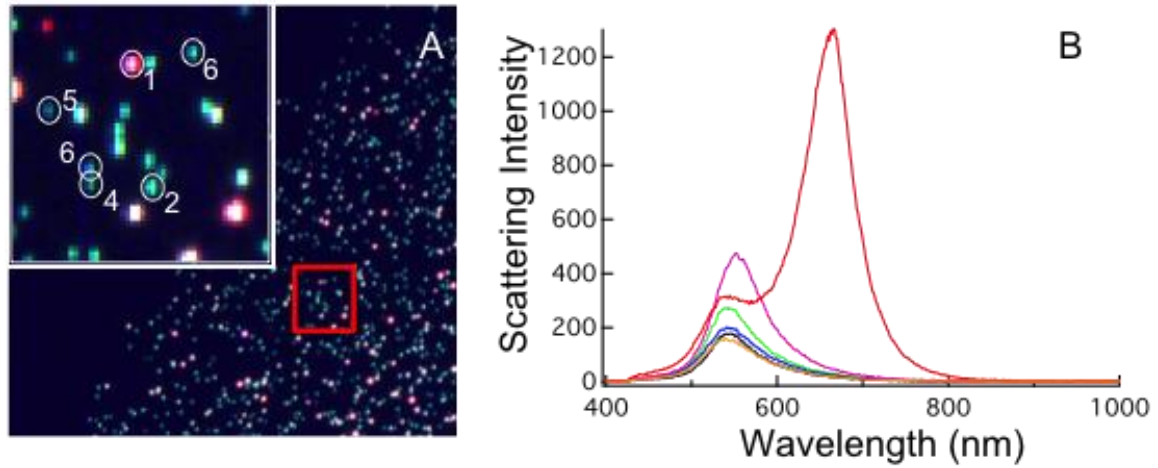
Nanoparticles were conjugated with a human IgG antibody using standard EDC coupling chemistry. Antibody conjugation was verified using dynamic light scattering and measuring the zeta-potential on the particles. The conjugated particles showed the expected 20 nm increase in hydrodynamic radius, and the zeta-potential was observed to become more negative following conjugation.

Hyperspectral dark field microscopy shows that we see different populations of nanoparticles after conjugation (Supporting Figure 1). In particular, we see a relatively uniform spectral response from what is believed to be single particles, represented by a scattering maximum at 545 nm. We also see particles that evince a more intense and slightly red-shifted plasmon that suggests two particles are weakly coupled and located within the diffraction-limited focus. There are also a small number of aggregates that evince a split scattering peak, with a red and blue shifted component at 665 and 538 nm, respectively. This split plasmon is consistent with reported models of plasmon coupling.<sup>5</sup> These results indicate that the color and intensity of particles observed in dark-field microscopy can guide experiments with increased resolution.

To identify the Raman peaks associated the antibody-conjugated nanoparticle, a conventional surface enhanced Raman spectrum was obtained for conjugated nanoparticle aggregates (Supporting Figure 2). Prominent peaks are observed at 550, 856, 930, 1007, 1135, 1240, 1370, 1455, and 1485  $\text{cm}^{-1}$  that can be largely attributed to aromatic amino acids.<sup>6-8</sup> Peaks at 856, 1139, 1182, 1277, and 1487  $\text{cm}^{-1}$  have been previously assigned to tyrosine in proteins<sup>6</sup> and in the anti-IgG antibody.<sup>8</sup> 1007  $\text{cm}^{-1}$  is a

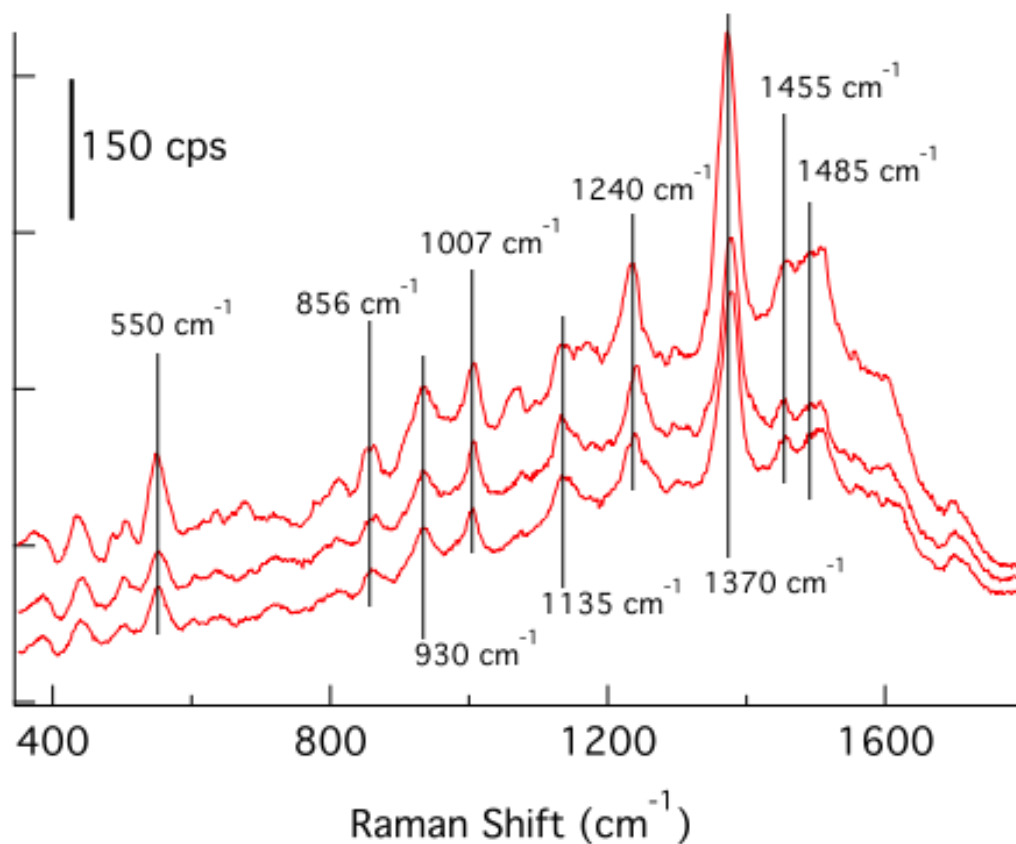
characteristic ring mode in phenylalanine and  $550\text{ cm}^{-1}$  is attributable to a trans-gauche-trans disulfide bond.<sup>6</sup> Tryptophan accounts for the remaining peaks at 930, 1370, 1455, and  $1485\text{ cm}^{-1}$ . The peaks observed in the SERS spectrum account for the spectrum observed for the isolated nanoparticle in Figure 2. Evidence of the antibody can also be observed in the spectra from the aggregated nanoparticles on the cell membrane (Figure 3).

Supporting Figure 1.



**Supporting Figure 1.** The dark field image of our 50 nm conjugated nanoparticles is shown in A. The inset is a blow-up of the area marked by the red box. The spectrum obtained from the circled particles are plotted in B. Isolated particles (e.g.- particles 3-6) show strong uniformity, while aggregated particles (e.g.- particle 1) are detected by their color and characteristic spectral profile. The red, magenta, green, black, orange, and purple traces correspond to particles 1, 2, 3, 4, 5, and 6, respectively.

Supporting Figure 2.



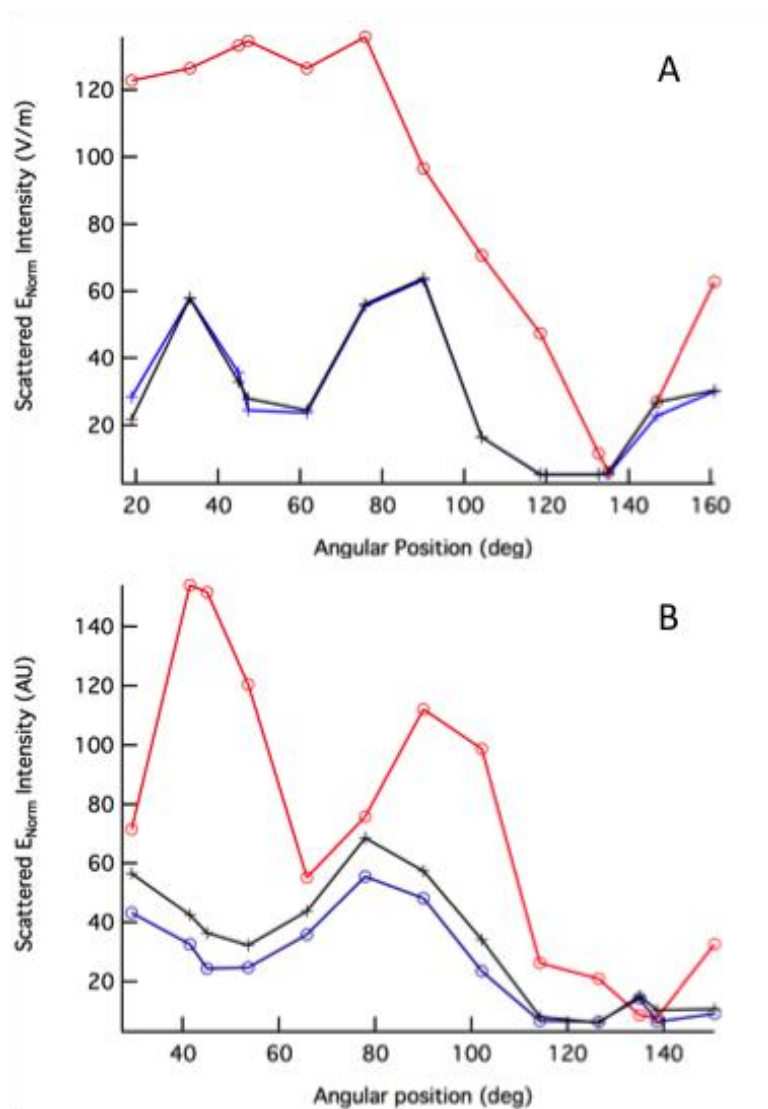
**Supporting Figure 2.** The SERS spectrum obtained from the IgG antibody-conjugated nanoparticles is shown. Three separate measurements are plotted to illustrate the reproducibility of the prominent features in the spectrum.



### FEM Calculations of Dipole coupling with an offset.

The “tip” was offset distances of +/- 20 nm along the y-axis in the plane of the target nanoparticle and moved laterally across to simulate tip scanning. Because the exact size of the tip is only approximately known, we performed simulations for a 100 nm and a 150 nm tip. In Figure 6 we notice that, for the majority of tip positions, the scattered electric field strength is greatest when the tip moves over the fixed nanoparticle. The magnitude of the scattered electric field reaches its maximum and its minimum at angular positions 45 and 135 degrees, respectively, as expected from the graphical illustrations given in Figure 5. The electric field strengths calculated for the offset positions are notably weaker, supporting the observation of the strong TERS enhancement in a single row of pixels. We believe that no spread of the enhancement is observed above or below the area where the tip passes directly over the fixed nanoparticle because the effective dipole coupling does not generate sufficient signal. In the simulation result for a 150 nm tip (supporting Figure 3), the offset measurements approach the in-line results at an angular position of approximately 80 degrees. Because we do not see corresponding enhancements in the experimental results at this angular position, we conclude that this is because the size of the tip is closer to 100 nm than 150 nm.

Supporting Figure 3.



**Supporting Figure 3:** The results of the COMSOL simulation are shown modeling the scattered electric field strength when the TERS tip scans over the fixed Au nanoparticle. The simulations were performed for a 100 nm tip (A) and a 150 nm Au tip (B) showing how nanoparticle asymmetry affects the observed coupling. Red traces denote the scattered field strength when the tip passes directly over the fixed nanoparticle and the blue and black traces denote the field strength the tip is displaced 20 nm above and below the nanoparticle, respectively.

## References:

1. S. L. Carrier, C. M. Kownacki, Z. D. Schultz, Protein-ligand binding investigated by a single nanoparticle TERS approach. *Chem. Commun.* 2011, 47. 2065-2067.
2. Z. D. Schultz, S. J. Stranick, I. W. Levin, Advantages and Artifacts of Higher Order Modes in Nanoparticle-Enhanced Backscattering Raman Imaging. *Anal. Chem.* 2009, 81. 9657-9663, DOI: 10.1021/ac901789w.
3. P. B. Johnson, R. W. Christy, Optical Constants of the Noble Metals. *Phys Rev B* 1972, 6. 4370-4379.
4. K. S. Youngworth, T. G. Brown, Focusing of high numerical aperture cylindrical-vector beams. *Optics Express* 2000, 7. 77-87.
5. W. S. Chang, L. S. Slaughter, B. P. Khanal, P. Manna, E. R. Zubarev, S. Link, One-Dimensional Coupling of Gold Nanoparticle Plasmons in Self-Assembled Ring Superstructures. *Nano Lett* 2009, 9. 1152-1157, DOI: 10.1021/nl803796d.
6. W. L. Peticolas, Raman spectroscopy of DNA and proteins. *Methods Enzymol.* 1995, 246. 389-416.
7. C.-H. Chuang, Y.-T. Chen, Raman scattering of L-tryptophan enhanced by surface plasmon of silver nanoparticles: vibrational assignment and structural determination. *Journal of Raman Spectroscopy* 2009, 40. 150-156, DOI: 10.1002/jrs.2097.
8. E. S. Grabbe, R. P. Buck, Evidence for a Conformational Change with Potential of Adsorbed Anti-IgG Alkaline-Phosphatase Conjugate at the Silver Electrode Interface Using SERS. *Journal of Electroanalytical Chemistry* 1991, 308. 227-237, DOI: 10.1016/0022-0728(91)85069-2.